EXPERIMENTS ON PROTON-PROTON SCATTERING BETWEEN 8 AND 26 GeV

A. N. Diddens, E. Lillethun, G. Manning,(*) A. E. Taylor(*), T. G. Walker(**), and A. M. Wetherell

CERN, Genève

(presented by A. E. Taylor)

1. INTRODUCTION

A series of measurements of $p-p$ elastic and near-elastic scattering have been made in the energy range 8 to 26 GeV. For some of the measurements CH_2 and C targets were used in the internal beam of the CERN proton synchrotron. In order to obtain the $p-p$ cross section, a subtraction method was used, based on the Be^7 activity produced in the targets. This technique was employed for several energies at scattering angles of 20 and 110 mrad and was similar to that reported previously for 56 and 60 mrad [1]. Cross sections have also been obtained from measurements of the scattering of an external proton beam from a liquid H_2 target for 5 energies in the range 12-26 GeV and for scattering angles of 10, 20, 30, 40 and 50 mrad. For all measurements a momentum analysis was made of the scattered particles in order to separate elastic and inelastic scattering.

The measurements of the differential elastic cross sections have covered a range of $-t$ values (square of four-momentum transfer) from 0.011 to 5.4 $(GeV/c)^2$ and s values (square of total C.M. energy) 18 to 52 $(GeV)^2$. The development of the structure found previously [1] in the near-elastic scattering has been followed from small $-t$ values up to 2 $(GeV/c)^2$.

2. EXTERNAL BEAM MEASUREMENTS

The experimental layout is shown in Fig. 1. The external beam was quasi-elastically scattered at an angle of 20 mrad from an internal PS target and was collimated to 1×6 cm at its exit from the shielding wall. Its intensity was $\sim 10^6$ protons/pulse and its divergence was 0.6 mrad in the horizontal plane and 2 mrad vertically. Momentum analysis of this beam gave typically 70% of the intensity concentrated in a band less than 200 MeV/c wide, with the remaining 30% in a low-momentum tail stretching to 1 GeV/c below the main peak.

The beam was monitored by two small scintillation counters in coincidence placed in the beam and its total intensity was obtained by scanning the counters across it.

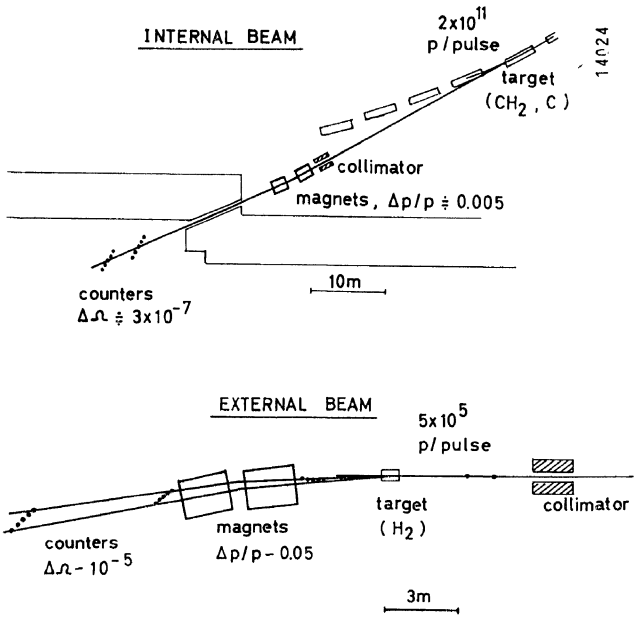

Fig. 1 Experimental layouts for external and internal beam measurements.

(*) On leave of absence from the Atomic Energy Research Establishment, Harwell, England.

(**) On leave of absence from the National Institute for Research in Nuclear Science. Harwell. England.

The beam was incident upon a liquid H_2 target of 1.26 g cm^{-2}. Protons scattered at angles of 10, 20, 30, 40 and 50 mrad were momentum analysed and detected simultaneously by a magnetic spectrometer involving five triple coincidence counter telescopes arranged as shown in Fig. 1. The momentum spectra were obtained by varying the magnetic field.

Results

The elastic differential cross sections were obtained by fitting the theoretical spectrometer resolution functions to the experimentally determined momentum spectra. Because of the poor momentum resolution it was possible for inelastic contributions to affect seriously the fitting procedure at the larger angles where the elastic cross sections were relatively small. To study the effects of such uncertainties the resolution functions were folded into spectra taken from the internal beam experiments in which the elastic and inelastic contributions were clearly separated. Comparison of the calculated and experimental spectra gave estimates of the possible errors in the elastic cross section from inelastic contributions; such errors were never more than 20%.

The elastic differential cross sections are given in Table I. The errors arise from uncertainties in estimating the incident flux and spectrum of protons, in alignment of counters and beam and, at the larger angles for the highest energies, in estimating the inelastic contamination as outlined above. Since it is of interest to determine both the t and the s dependence of the cross section, the errors have been separated into relative errors for each energy, and absolute errors.

TABLE I

Elastic $p-p$ Cross Sections

	Θ_{lab} mrad	$\Theta_{c.m.}$ degrees	$-t$ $(GeV/c)^2$	$\left(\frac{d\sigma}{d\Omega}\right)_{el}$ b/ster	$\left[\left(\frac{4\pi}{k\sigma_T}\right)^2 \frac{d\sigma}{d\Omega}\right]_{c.m.}$	Relative errors within one energy, %	Absol. errors %
$p_0 = 12.1$ GeV/c	8.8	2.66	0.011	4.03	1.10	11	19
$\gamma = 12.85$	19.1	5.73	0.052	2.60	0.70	8	16
$s = 24.4$ GeV^2	29.1	8.72	0.121	1.20	0.33	5	16
	39.1	11.75	0.219	0.58	0.16	5	16
	49.1	14.7	0.342	0.20	0.057	6	16
$p_0 = 15.5$ GeV/c	8.9	3.02	0.019	5.79	0.96	12	18
$\gamma = 16.5$	18.9	6.40	0.086	2.63	0.44	10	15
$s = 30.8$ GeV^2	28.9	9.71	0.195	0.92	0.16	6	15
	38.9	13.25	0.364	0.22	0.038	8	16
	48.9	16.50	0.563	0.036	0.0059	15	21
$p_0 = 18.6$ GeV/c	10.8	4.0	0.040	7.93	0.87	12	22
$\gamma = 19.8$	20.8	7.7	0.148	2.46	0.28	6	20
$s = 36.6$ GeV^2	30.8	11.3	0.323	0.46	0.051	6	20
	40.8	15.1	0.561	0.059	0.0068	15	24
	50.8	18.8	0.866	0.009	0.0011	20	27
$p_0 = 21.4$ GeV/c	8.3	3.29	0.032	8.65	0.75	12	21
$\gamma = 22.8$	18.6	7.30	0.155	1.95	0.175	8	18
$s = 41.9$	28.6	11.18	0.364	0.29	0.025	7	19
	38.6	15.30	0.680	0.024	0.0022	10	20
	48.6	19.0	1.055	0.0020	0.00018	30	34
$p_0 = 26.2$ GeV/c	9.5	4.21	0.064	11.3	0.65	13	22
$\gamma = 27.9$	19.5	8.60	0.268	1.31	0.078	7	21
$s = 50.9$	29.5	12.88	0.596	0.072	0.0043	10	22
	39.5	17.03	1.042	0.0041	0.00025	25	28

The values of $\Theta_{c.m.}$ and $-t$ for $p_0 = 18.6$ GeV/c have been corrected since the conference.

3. INTERNAL BEAM MEASUREMENTS

The technique used with the internal CH_2 and C targets has been described before [1] and therefore only the results are reported here. Since the beam scattered at 20 mrad passed through the walls of the vacuum chamber and was subject to strong focusing in the fringing field of the PS, it is impossible to obtain reliable values of the elastic cross sections for this scattering angle. It is possible, however, to compare the near-elastic scattering with the elastic scattering and observe the change in its structure for different energies. The spectra can be put on an absolute scale by normalizing to the elastic cross sections found in the external beam measurements. These objections do not apply to the 110 mrad data from which the absolute cross sections were obtained by comparison with the Be^7 activity induced in the targets.

A recent determination of the C^{12} $(p, 3p3n)$ Be^7 cross section [2] gave a value of 7.7 ± 0.4 mb at 28 GeV compared with the value of 11 mb assumed in the previously reported results of 56 mrad. In determining the cross sections at 110 mrad this new value has been used and the cross sections for 56 mrad used here have been changed accordingly. Small changes in the 56 mrad cross sections at the largest and at the two smallest momentum transfers have been made as the result of a reconsideration of the subtraction procedure.

4. ELASTIC DIFFERENTIAL CROSS SECTIONS

The values of the differential cross sections obtained from the internal target measurements are given in Table II, and shown in Fig. 2 together with those from the external beam measurements. This diagram shows the dependence on $-t$ of $\left[\left(\frac{4\pi}{k\sigma_T}\right)^2 \frac{d\sigma}{d\Omega}\right]_{c.m.}$

Within the accuracy of the data, the two smallest momentum transfer cross sections for all five energies

TABLE II

Elastic $p-p$ Cross Sections

Θ_{lab} mrad	$(P_0)_{lab}$ GeV/c	$s/2M^2$	$-t$ (GeV/c)^2	$(d\sigma/d\Omega)_{lab}$ mb/sr	$\Theta_{c.m.}$ degrees	$\left(\frac{d\sigma}{d\Omega}\right)_{c.m.}$ mb/sr	$\left[\left(\frac{4\pi}{k\sigma_T}\right)^2 \frac{d\sigma}{d\Omega}\right]_{c.m.}$
56.5	12.99	14.8	0.524	45	17.5	1.6	$1.1\ 10^{-2}$
56.5	15.89	17.9	0.783	10	19.2	0.30	$1.6\ 10^{-3}$
56.5	17.30	19.4	0.925	4.5	20.0	0.13	$6.4\ 10^{-4}$
56.5	17.75	19.9	0.978	5.3	20.2	0.15	$7.0\ 10^{-4}$
56.5	18.69	20.9	1.084	1.5	20.7	0.039	$1.7\ 10^{-4}$
56.5	19.56	21.9	1.184	0.53	21.2	0.013	$5.7\ 10^{-5}$
56.5	19.75	22.1	1.206	0.90	21.3	0.022	$9.5\ 10^{-5}$
56.5	19.91	22.2	1.221	0.54	21.4	0.013	$5.6\ 10^{-5}$
56.5	21.88	24.3	1.474	0.28	22.3	0.0062	$2.5\ 10^{-5}$
56.5	22.74	25.2	1.590	0.24	22.6	0.0050	$1.9\ 10^{-5}$
56.5	26.02	28.7	2.071	0.10	24.2	0.0019	$6.3\ 10^{-6}$
60.5	18.29	20.5	1.184	0.56	21.9	0.015	$7.0\ 10^{-5}$
60.5	27.83	30.6	2.68	0.026	26.6	0.00047	$1.5\ 10^{-6}$
110	8.94	10.5	0.91	2.75	28.4	0.14	$1.45\ 10^{-3}$
110	11.28	13.0	1.43	0.31	31.5	0.013	$1.08\ 10^{-4}$
110	13.98	15.9	2.17	0.12	34.6	0.0044	$2.88\ 10^{-5}$
110	15.96	18.0	2.80	0.040	36.7	0.0013	$7.68\ 10^{-6}$
110	18.97	21.1	3.86	0.0055	39.5	0.00016	$7.55\ 10^{-7}$
110	21.46	23.9	4.91	0.0011	41.8	0.00003	$1.2\ 10^{-7}$
110	22.92	25.4	5.55	<0.0007(*)	43.0	<0.00002(*)	$<7\ 10^{-8}$(*)

The error in the differential cross-section is estimated to be $\pm 50\%$.

Θ, P_0 are the scattering angle and incoming momentum. s is the square of the total c.m. energy, M the nucleon mass and $-t$ of the square the four-momentum transfer. σ_T is the total $p-p$ cross-section and k the c.m. wave number.

*) 95% confidence level.

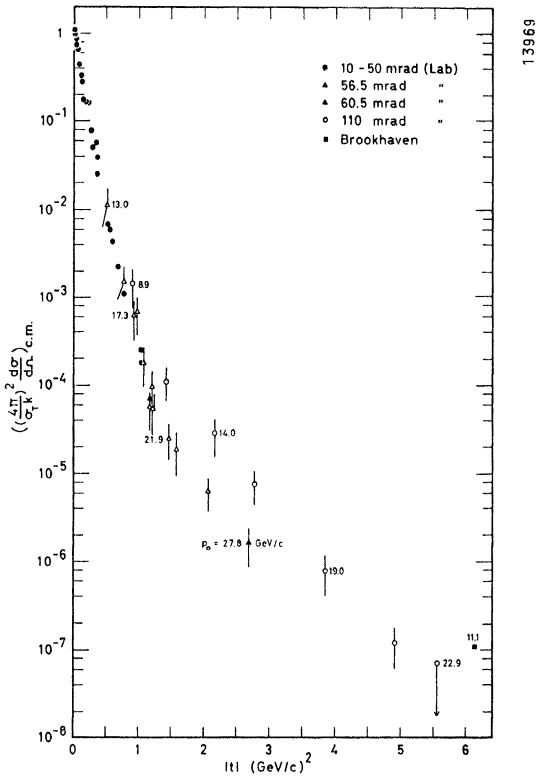

Fig. 2 Elastic differential cross sections normalized to the forward scattering cross section given by the optical theorem and plotted as a function of $-t$.

of the external beam experiment extrapolate to an average value of 1.2 ± 0.2 at $t = 0$. As this value is not significantly different from unity, the value given by the optical theorem for a purely imaginary scattering amplitude, one may put

$$\left(\frac{4\pi}{k\sigma_T}\right)^2 \frac{d\sigma}{d\Omega} = \left(\frac{d\sigma}{dt}\right) \Big/ \left(\frac{d\sigma}{dt}\right)_{t=0} .$$

This initial slope of the curve corresponds to putting

$$\frac{d\sigma}{dt} = \left(\frac{d\sigma}{dt}\right)_{t=0} \exp(+10t)$$

whereas the initial slope predicted by Amati *et al.*[3], from the " strip approximation ", is $\exp(+12.5t)$.

The smallest cross section obtained at 110 mrad and 21.9 GeV from the internal beam experiment corresponds to 2×10^{-32} cm^2/st at 43° in the C.M. system. In this region the cross section still appears to be decreasing but with a slope $\approx 1/5$ of that at smaller momentum transfers.

For increasing values of s there is a definite shrinking of the width of the diffraction pattern and this is shown most clearly in Fig. 3. Here the normalized cross section $\left(\frac{d\sigma}{dt}\right) \Big/ \left(\frac{d\sigma}{dt}\right)_{t=0}$ is plotted against $S/2M^2$ for various values of $-t$. The cross sections related to the external beam measurements were obtained by interpolation, while for larger values of $-t$ direct cross sections from the internal beam measurements are plotted. Also included in the figure are interpolated data for representative lower energies [4, 5].

If, as has been suggested [6, 7, 8, 9] by the Regge pole theory of strong interactions, the cross section can be put in the form

$$\left(\frac{d\sigma}{dt}\right) \Big/ \left(\frac{d\sigma}{dt}\right)_{t=0} = F(t)\left(\frac{S}{2M^2}\right)^{2(\alpha(t)-1)}$$

then both the functional dependence of F and α upon t can be obtained from Fig. 3. The slope of $\ln\left[\left(\frac{d\sigma}{dt}\right) \Big/ \left(\frac{d\sigma}{dt}\right)_{t=0}\right]$ with $\ln(S/2M^2)$ gives the value of $2(\alpha(t)-1)$ and the intercept at $S/2M^2 = 1$ gives $\ln F(t)$. For $0<-t<1.0$ (GeV/c)^2, it is found that

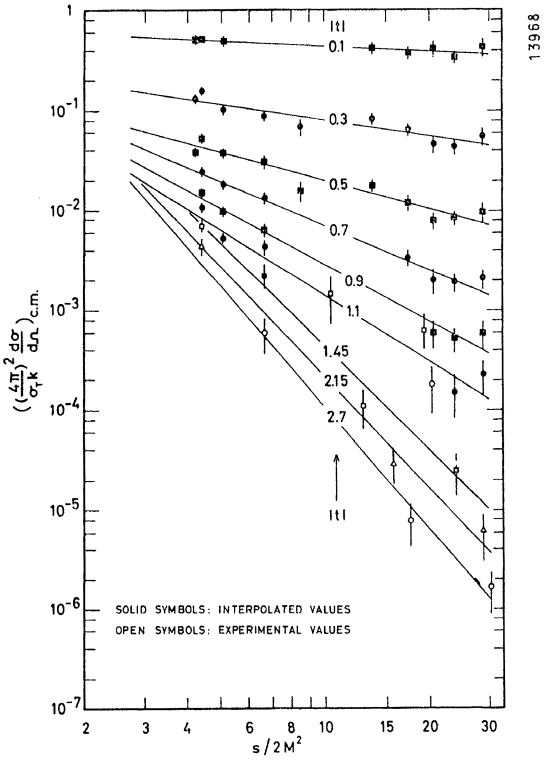

Fig. 3 Normalized elastic differential cross sections for constant t values plotted against $S/2M^2$.

a single value of $\alpha(t)$ and $F(t)$ can be used in the energy range 3-30 GeV. For larger momentum transfers α and F can only be obtained by comparison of either one low-energy and one or two high-energy cross sections or by comparison of the two internal beam measurements at 56 and 110 mrad. The parameters thus obtained have large uncertainties.

The dependence of α on $-t$ is given in Fig. 4, which is split into two parts showing the $\alpha(t)$ obtained by taking all the data in Fig. 3 and that found by taking only those at energies above 9 GeV in the lab system. In the first case the function is quite well determined; it decreases essentially linearly from 1 to zero at $-t \approx 1.0$ (GeV/c)^2 and approaches -1 for larger momentum transfers. The determination of $\alpha(t)$ from the high-energy data alone is poor, but

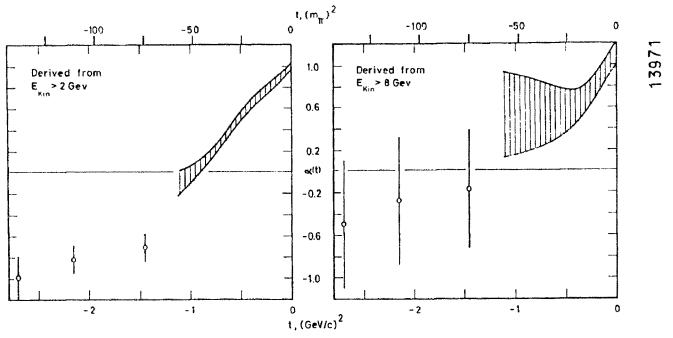

Fig. 4 The t dependence of the Regge term $\alpha(t)$ derived from Fig. 3.
(a) shows the function obtained by taking all the data in Fig. 3;
(b) gives the function found by using only the data taken at energies above 9 GeV in the lab system.

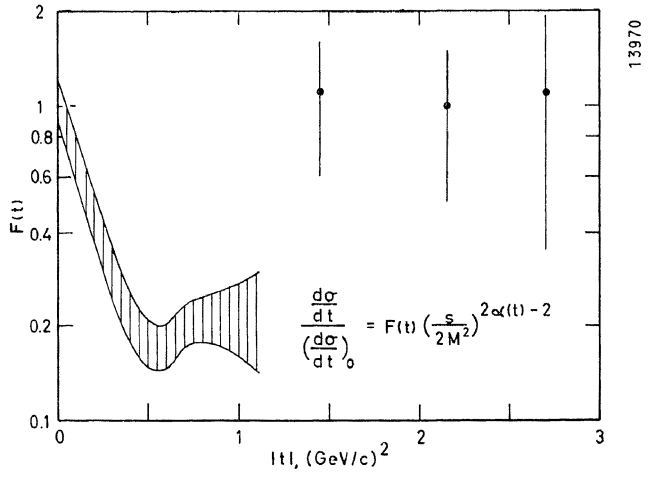

Fig. 5 The t dependence of $F(t)$ derived from Fig. 3.

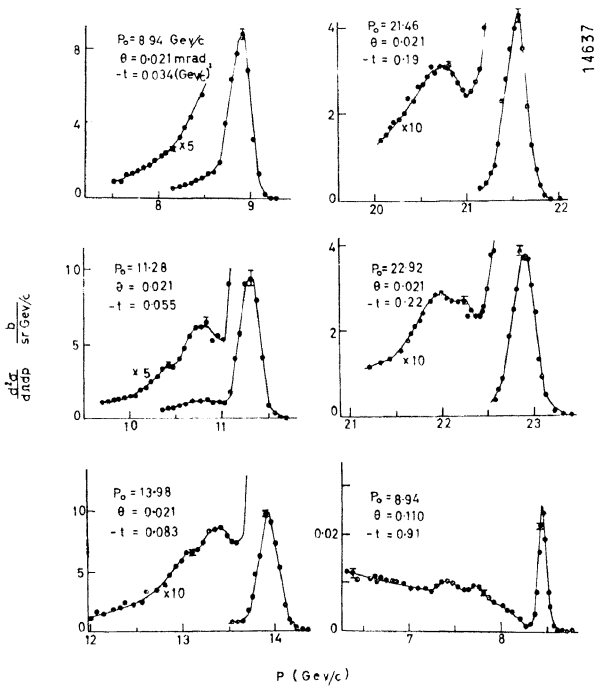

Fig. 6 Various momentum spectra exhibiting the development of the structure in the inelastic scattering.

the same general shape is found. There appears to be a tendency for the function at higher momentum transfers to remain somewhat higher than is apparent from the $\alpha(t)$ determined by data from the whole energy range.

The experimentally determined function $F(t)$ as given in Fig. 5 was obtained using the data from the whole energy range.

Inelastic scattering

In the previously reported inelastic spectra for $p-p$ scattering at 56 mrad [1], a double bump structure was observed. This is again evident in the spectra measured at 20 and 110 mrad, examples of which are shown in Fig. 6. As before, the positions of the bumps correspond very closely in the missing mass to the second and third $\pi-p$ resonances; the actual values obtained for the missing masses were 1.51 ± 0.01 and 1.69 ± 0.01 GeV. The spectra show no evidence for the production of a mass corresponding to the (3/2, 3/2) state, which would appear as a bump about 300 MeV/c below the elastic peak.

It is clear that for the smallest value of $-t$ (0.03 (GeV/c)^2) there is little evidence of any structure

and the relative amount of near-elastic scattering is much lower. On increasing the momentum transfer to $-t = 0.055\,(\mathrm{GeV/c})^2$ structure now appears. Drell and Hiida's interpretation [10] of this structure in terms of a peripheral interaction in which the incident proton is diffracted by a virtual pion implies that the separation of the bump should change from 0.35 to 1.5 GeV/c for the $-t$ values where structure is seen. However, such an explanation needs to be supplemented to produce the double bump structure at constant separation from the elastic peak.

The dependence in magnitude of this structure on $-t$ is shown in Figs. 7a and 7b where two different assumptions have been made. In Fig. 7a the whole cross section below the structure is compared with the elastic cross section, whereas in Fig. 7b it was assumed that this structure was sitting on top of a background. Under the first assumption, there is an approximately constant ratio for $-t<0.3$ $(\mathrm{GeV/c})^2$ and then a rather rapid increase, roughly as t^2. In the second case the rate of increase of the ratio for $-t>0.3$ $(\mathrm{GeV/c})^2$ is about the same as before but the magnitude of the ratio is about a factor of 10 less. Although the elastic cross-section changes by a factor

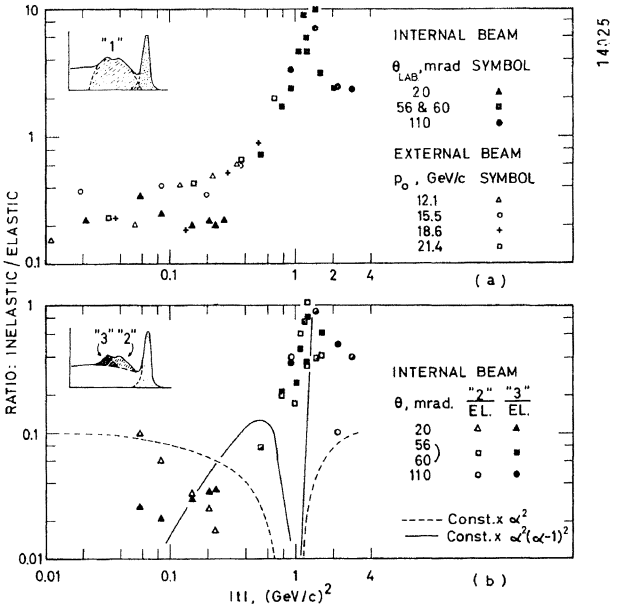

Fig. 7 (a) Ratio to the elastic of the cross section associated with the structure in the inelastic scattering when no background effects are assumed;

(b) Ratio to the elastic of the cross section associated with the structure in the inelastic scattering when the structure is assumed to sit upon the background indicated.

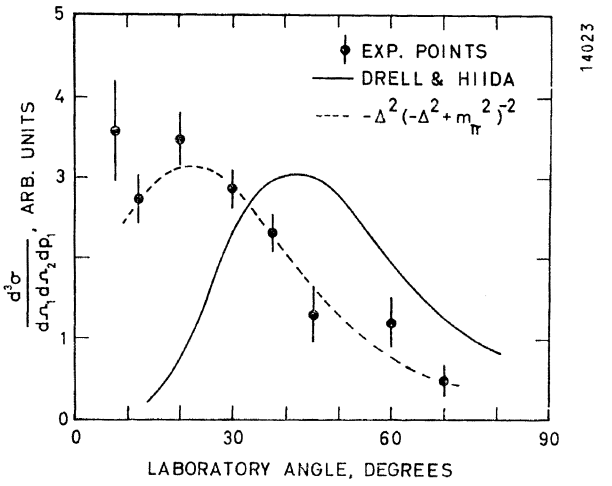

Fig. 8 Angular correlation between recoiling charged particles and a proton scattered at 20 mrad with an inelasticity of ≈ 1 GeV.

10^5 in this range, these ratios have only changed by a factor 30.

The constancy of the separation of the double bump structure and the equality in missing mass with the second and third $\pi-p$ resonances is suggestive of the formation of nucleon isobars. From a general consideration of a Regge pole theory of the production of excited $T = \frac{1}{2}$ nucleon states, Frautschi *et al.* [9] obtained a dependence on t of the ratio of inelastic to elastic scattering which is shown in Fig. 7. In this theory the excited states are produced by an inelastic diffraction process and provided that the isotopic spin cannot change in diffractive processes, suppression of the (3/2, 3/2) state is guaranteed. This remark is true also for the diagram calculated by Drell and Hiida [10] if a final state interaction leads to the excited states.

The model of Drell and Hiida, calculated without a final state interaction, gives a definite prediction for the angular correlation of the recoiling system. A rough measurement was made of the angular correlation between the recoiling charged particles and protons scattered at 20 mrad with an inelasticity ≈ 1 GeV/c. The results are shown in Fig. 8, where it is apparent that the simple model predicts a peaking at too large an angle. Whether the inclusion of final state interaction would alter the correlation as well as producing the double bump structure is not yet known. The correlation is not inconsistent with the direct formation of nucleon isobars however.

LIST OF REFERENCES

1. Cocconi, G., Diddens, A. N., Lillethun, E., Manning, G., Taylor, A. E., Walker, T. G., and Wetherell, A. M. Phys. Rev. Letters *7*, 450 (1961).
2. Cuming, J. B., Friedlander, G., Hudis, J., and Paskanzer, A. M., BNL 6034.
3. Amati, D., Fubini, S., Stanghellini, A., and Tonin, M. Nuovo Cimento *22*, 569 (1961).
4. Chadwick, G. B., Collins, G. B., Duke, P. J., Fujii, T., Hien, N. C., and Turkot, F. To be published (1962). We are grateful to this group for allowing us to use their data before publication.
5. Cork, B., Wenzel, W. A., and Causey, G. W., Phys. Rev. *107*, 859 (1957).
6. Lovelace, C., Proceedings Aix-en-Provence Conference II, 128, report by S. D. Drell. (1961).
7. Chew, G. F., and Frautschi, S. C. Phys. Rev. Letters *7*, 394 (1961).
8. Frautschi, S. C., Gell-Mann, M., and Zachariasen, F. (To be published) 1961.
9. Gribov, V. M., Soviet Physics — JETP *14*, 478 (1962).
10. Drell, S. D., and Hiida, K., Phys. Rev. Letters *7*, 199 (1961).

ON THE DIFFRACTION ELASTIC p-p SCATTERING AT 6 GeV AND 10 GeV

B. Bekker, L. Kirillova, A. Nomofilov, V. Nikitin, V. Pantuev, V. Sviridov, L. Strunov, M. Khachaturian and M. Shafranova

Joint Institute for Nuclear Research, Dubna

(presented by I. Chuvilo)

The aim of this investigation is the measurement and analysis of differential cross-sections of elastic $p-p$ scattering at the proton energies 6 GeV and 10 GeV. The knowledge of these cross-sections with sufficient accuracy permits us to calculate the universal Regge function $L(t)$. The scheme of the experiment is shown on Fig. 1.

A thin polyethylene target of 2 micron thickness was used in the internal proton beam of the synchrophasotron, to reduce the energy spread and multiple Coulomb scattering. The recoil protons were detected by nuclear emulsions.

In these experimental conditions, there exists a possibility of measuring the differential cross-section of elastic $p-p$ scattering with good accuracy. The angular resolution of the experiment is less than 3 milliradian.

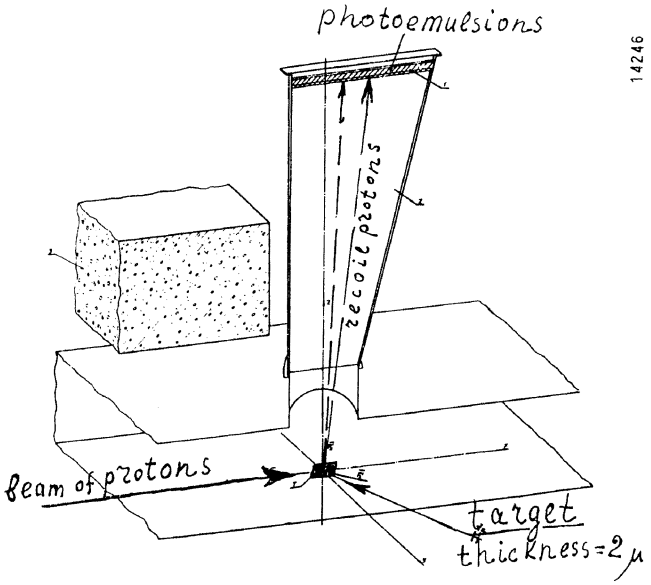

Fig. 1 Scheme of the experiment.